Table 1 continued

Characteristics	Number of patients (total = 66)	3-year RFS rate (%)	Univariate analysis p value[a]	Multivariate analysis	
				Hazard ratio (95 % CI)	p value[b]
Tumor differentiation					
Well/moderate	50	33.6	0.867		
Poorly	16	40.9			
EGFR mutation					
Mutant	18	41.6	0.604		
Wild-type	48	33.6			
KRAS mutation					
Mutant	6	22.2	0.659		
Wild-type	60	36.9			
Adjuvant chemotherapy					
Yes	33	49.8	0.021†	1	0.028†
No	33	20.2		2.05 (1.08–3.87)	

PS performance status, *CEA* preoperative serum carcinoembryonic antigen level, *LNR* lymph node ratio

† Denotes significance

[a] Log-rank test

[b] Cox's proportional hazard model

less than 10 nodes were harvested were also included in this study because all underwent dissection of all the nodal stations mentioned above. The LNR was defined as the number of involved nodes divided by the total number of nodes removed [22].

DNA extraction and mutational analysis

After surgical removal, a portion of each sample was immediately frozen and stored at −80 °C prior to DNA extraction. Genomic DNA was extracted from a 3–5 mm cube of tumor tissue using DNA Mini Kits (Qiagen, Hilden, Germany), and subsequently diluted to a concentration of 20 ng/μL. *EGFR* and *KRAS* mutations in lung cancer tissues were analyzed via PNA-enriched sequencing, as described previously [23–25].

Statistical analysis

The recurrence-free survival (RFS) was defined as the time between the date of resection and the date of the first recurrence of lung cancer or the date of death from any cause. Patients without recurrence were censored from the analysis at the time of the last negative follow-up. The length of the recurrence-free period was measured from the date of surgery to the date of the first recurrence or the last follow-up. The recurrence-free proportion (RFP) was defined as the ratio of the patients who were free from recurrence. Patients without recurrence were censored from the analysis at the time of the last negative follow-up, and patients who died without evidence of recurrence were also censored.

To determine the appropriate prognostic SUV_{max} and LNRs, patients were subdivided into two cohorts via receiver operating characteristic (ROC) curve analyses. In univariate analyses, the RFS rate and RFP were estimated by the Kaplan–Meier method, and among-group survival differences were compared using the log-rank test. Multivariate analyses were performed using Cox's proportional hazard model. The Chi square test was performed for comparison of the relationship between the SUV_{max}, the LNR, and clinicopathological features.

All reported p values were two-sided, and the significance level was set at $p < 0.05$. All analyses were performed using the SPSS version 20.0 software program (Dr. SPSS II for Windows, standard version 20.0; SPSS Inc., Chicago, IL, USA).

Results

Patient characteristics

The characteristics of all 66 patients with lymph node metastases are listed in Supplementary Table 1. The median patient age was 69 years, and 46 males were included. The histological findings were as follows: adenocarcinoma ($n = 46$), squamous cell carcinoma ($n = 18$), large cell carcinoma ($n = 1$), and large cell neuroendocrine carcinoma ($n = 1$). The SUV_{max} ranged from 1.19 to 17.30 (median 3.5). A total of 27 patients were of pathological N1 and 39 were of N2. *EGFR* mutations were detected in 18 patients (27 %) and 33 (50 %) received adjuvant chemotherapy.

Table 2 Prognostic factors of the recurrence-free proportion

Characteristics	*Number of patients (total = 66)*	*3-year RFP (%)*	*Univariate analysis p value*[a]	*Multivariate analysis*	
				Hazard ratio (95 % CI)	*p* value[b]
Age (years)					
<70	35	39.7	0.987		
≥70	31	39.3			
Sex					
Male	46	41.6	0.402		
Female	20	34.3			
PS					
0	58	40.6	0.530		
1	8	26.3			
Smoking history					
Never	16	43.8	0.837		
Ever	50	37.7			
CEA (ng/mL)					
≤5.0	43	40.9	0.446		
>5.0	23	36.6			
Laterality					
Right	39	41.1	0.742		
Left	27	37.3			
Clinical nodal staging					
cN0	41	38.4	0.971		
cN1	16	38.5			
cN2	9	44.4			
Histology					
Adenocarcinoma	46	43.7	0.337		
Non-adenocarcinoma	20	29.5			
SUV_{max} of the tumor					
≤6.5	23	74.1	<0.001[†]	1	0.001[†]
>6.5	43	23.0		4.48 (1.79–11.20)	
Pathological T status					
pT1	12	75.0	0.017[‡]	1	0.427
pT2–4	54	29.6		1.65 (0.48–5.66)	
Pathological nodal involvement					
pN1	27	53.3	0.039[§]	1	0.750
pN2	39	31.6		1.09 (0.65–1.83)	
LNR					
≤0.12	30	62.6	<0.001[†]	1	0.055
>0.12	36	23.0		2.86 (0.98–8.39)	
Lymphatic permeation					
Ly (−)	5	75.0	0.126		
Ly (+)	61	37.0			
Vascular invasion					
V (−)	14	29.6	0.593		
V (+)	52	41.8			
Pleural invasion					
PL (−)	25	50.6	0.147		
PL (+)	41	32.2			

Table 2 continued

Characteristics	Number of patients (total = 66)	3-year RFP (%)	Univariate analysis p value[a]	Multivariate analysis	
				Hazard ratio (95 % CI)	p value[b]
Tumor differentiation					
Well/moderate	50	37.5	0.871		
Poorly	16	43.6			
EGFR mutation					
Mutant	18	41.6	0.872		
Wild-type	48	38.4			
KRAS mutation					
Mutant	6	44.4	0.897		
Wild-type	60	39.0			
Adjuvant chemotherapy					
Yes	33	53.2	0.047†	1	0.062
No	33	22.5		1.89 (0.97–3.68)	

RFP recurrence-free proportion, *PS* performance status, *CEA* preoperative serum carcinoembryonic antigen level, *LNR* lymph node ratio

† Denotes significance

[a] Log-rank test

[b] Cox's proportional hazard model

Supplementary Figure 2A shows the overall survival (OS) curve. The median follow-up time for surviving patients was 28.8 months. The overall 5-year survival rate after surgery was 47.2 %. The RFS curve is shown in Supplementary Figure 2B. The recurrence-free 5-year survival rate was 27.9 %.

Recurrence-free survival, recurrence-free proportion, and independent prognostic factors

Supplementary Figure 3 shows an ROC curve identifying optimal cut-off values for the LNR and the SUV_{max} in predicting lung cancer recurrence. The ROC areas under the curve were 0.683 ($p = 0.013$) for the LNR and 0.694 ($p = 0.007$) for the SUV_{max}, and the cut-off values were determined to be 0.12 for the LNR and 6.5 for the SUV_{max}.

A univariate analysis showed that the tumor SUV_{max}, pathological T status, the LNR, and administration of adjuvant chemotherapy were significant prognostic factors regarding the RFS (Table 1). A multivariate analysis revealed that a tumor SUV_{max} higher than 6.5, an LNR over 0.12, and lack of adjuvant chemotherapy were significant, independent predictors of a poorer RFS [SUV_{max} >6.5: hazard ratio (HR) 3.88, $p = 0.002$; LNR >0.12: HR 2.18, $p = 0.023$; adjuvant chemotherapy: HR 2.05, $p = 0.028$] (Table 1).

We also determined the RFP focusing exclusively on lung cancer recurrence (Table 2). A univariate analysis showed that the tumor SUV_{max}, pathological T status, pathological nodal stage, the LNR, and adjuvant chemotherapy were significant prognostic factors regarding the RFP (Table 2). A multivariate analysis revealed that a tumor SUV_{max} greater than 6.5 was a significant, independent predictor of relapse (max SUV >6.5: HR 4.48, $p = 0.001$) (Table 2). Although significance was not attained, the LNR and adjuvant chemotherapy also exerted marginally significant prognostic impacts on recurrence ($p = 0.055$ and $p = 0.062$, respectively). Regarding the OS, the tumor SUV_{max}, pathological T status, *EGFR* mutation, and *KRAS* mutation were significant prognostic factors according to the univariate analysis. However, no independent significant factor of the OS was evident upon the multivariate analysis (data not shown).

Table 3 shows the relationships between clinicopathological features and the two independent prognostic factors (the SUV_{max} and the LNR). The SUV_{max} was significantly associated both with the histology and pathological T status, and the LNR exhibited significant relationships with sex, pathological nodal involvement, and lymphatic permeation.

Recurrence-free survival by independent prognostic factors

The RFS curves stratified by the numbers of the two independent risk factors, i.e., an SUV_{max} higher than 6.5 and an LNR over 0.12, are shown in Fig. 1a. All among-group survival differences were significant. The prognosis of the no-risk-factor group was optimal (3- and 5-year RFS rates were both 91.7 %), whereas that of the two-risk-factor group was extremely poor (3- and 5-year RFS rates were 12.0 and 6.0 %, respectively). The RFP curves drawn by reference to the numbers of the same

Table 3 Relationship between the SUV_{max}, LNR, and clinicopathological features

Variables	*N*	SUV max		*p* value[a]	LNR		*p* value[a]
		≤6.5 (*N* = 23)	>6.5 (*N* = 43)		≤0.12 (*N* = 30)	>0.12 (*N* = 36)	
Age (years)							
<70	35	13	22	0.678	15	20	0.652
≥70	31	10	21		15	16	
Sex							
Male	46	15	31	0.562	25	21	0.028[†]
Female	20	8	12		5	15	
PS							
0	58	22	36	0.157	26	32	0.783
1	8	1	7		4	4	
Smoking history							
Never	16	7	9	0.391	6	10	0.463
Ever	50	16	34		24	26	
CEA (ng/mL)							
≤5.0	43	17	26	0.275	21	22	0.450
>5.0	23	6	17		9	14	
Laterality							
Right	39	15	24	0.459	18	21	0.891
Left	27	8	19		12	15	
Clinical nodal staging							
cN0	41	18	23	0.082	20	21	0.074
cN1	16	2	14		9	7	
cN2	9	3	6		1	8	
Histology							
Adenocarcinoma	46	21	25	0.005[†]	19	27	0.304
Non-adenocarcinoma	20	2	18		11	9	
SUV_{max} of the tumor							
≤6.5	23	–	–		12	11	0.423
>6.5	43	–	–		18	25	
Pathological T status							
pT1	12	8	4	0.011[†]	8	4	0.103
pT2–4	54	15	39		22	32	
Pathological nodal involvement							
pN1	27	8	19	0.459	24	3	<0.001[†]
pN2	39	15	24		6	33	
Lymphatic permeation							
Ly (−)	5	3	2	0.220	5	0	0.011[†]
Ly (+)	61	20	41		25	36	
Vascular invasion							
V (−)	14	4	10	0.579	9	5	0.111
V (+)	52	19	33		21	31	
Pleural invasion							
PL (−)	25	12	13	0.080	15	10	0.064
PL (+)	41	11	30		15	26	
Tumor differentiation							
Well/moderate	50	18	32	0.729	24	26	0.463
Poorly	16	5	11		6	10	

Table 3 continued

Variables	*N*	SUV max		*p* value[a]	LNR		*p* value[a]
		≤6.5 (*N* = 23)	>6.5 (*N* = 43)		≤0.12 (*N* = 30)	>0.12 (*N* = 36)	
EGFR mutation							
Mutant	18	8	10	0.316	6	12	0.226
Wild-type	48	15	33		24	24	
KRAS mutation							
Mutant	6	2	4	0.935	3	3	0.815
Wild-type	60	21	39		27	33	

PS performance status, *CEA* preoperative serum carcinoembryonic antigen level, *LNR* lymph node ratio

† Denotes significance

[a] Pearson's Chi square test

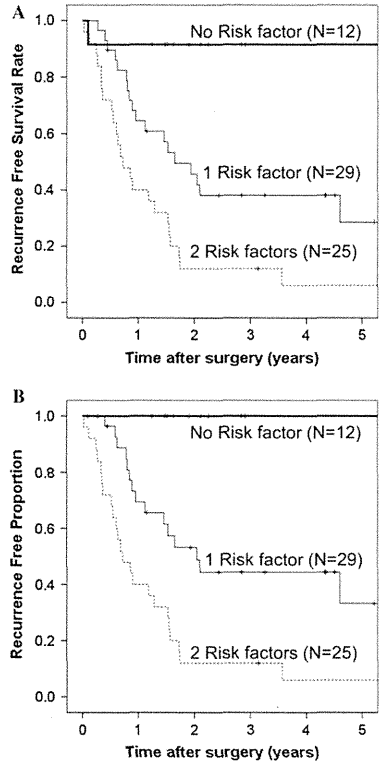

P-values in survival difference		
		P-value※
No RF vs	1 RF	0.01
	2 RFs	< 0.001
1 RFs vs	2 RFs	0.005

※ : by log-rank test. RF: risk factor

P-values in survival difference		
		P-value※
No RF vs	1 RF	0.005
	2 RFs	< 0.001
1 RFs vs	2 RFs	0.001

※ : by log-rank test. RF: risk factor

Fig. 1 Recurrence-free survival curves stratified by two independent risk factors, an SUV_{max} higher than 6.5 and an LNR higher than 0.12, are shown (**a**). The survival differences among all groups were significant. The prognosis of the no-risk-factor group was optimal (in terms of the 3- and 5-year RFS rates: both 91.7 %), whereas that of the one-risk-factor group was intermediate (3- and 5-year RFS rates: 38.1 and 28.6 %, respectively), and that of the two-risk-factor group was extremely poor (3- and 5-year RFS rates: 12.0 and 6.0 %, respectively). As the number of risk factors increased, the survival rates decreased. Recurrence-free proportion curves by the numbers of the same risk factors are shown in **b**. The survival differences were similar to those exhibited by the RFS curves, and all among-group survival differences were significant. All patients with no risk factors remained relapse-free during the follow-up

risk factors are shown in Fig. 1b. The survival differences were similar to those revealed by the RFS curves, and all among-group survival differences were significant. All patients with no risk factors remained relapse-free during the follow-up.

Figure 2 shows the RFS curves according to the administration (or not) of adjuvant chemotherapies in various groups differing in the numbers of risk factors. Although no significant survival difference was evident between the no-risk-factor group (Fig. 2a) and the one-risk-factor group

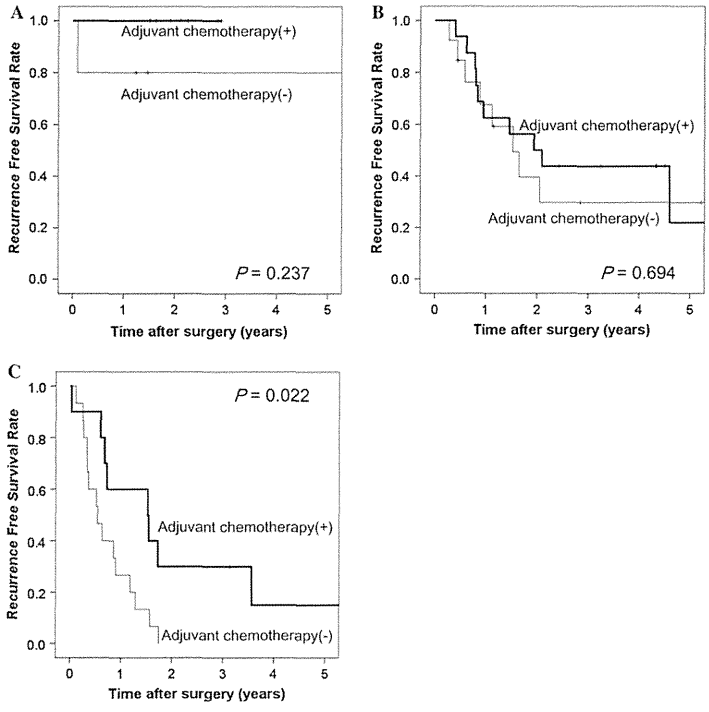

Fig. 2 Recurrence-free survival curves by treatment or not with adjuvant chemotherapies in terms of the numbers of risk factors present (**a** no risk factor, **b** one risk factor, **c** two risk factors). Although no significant survival difference was evident between the no-risk-factor group ($p = 0.237$, **a**) and the one-risk-factor group ($p = 0.694$, **b**), the prognoses of patients given adjuvant chemotherapies were better than others. In particular, in the two-risk-factor group, the survival difference was significant ($p = 0.022$, **c**)

(Fig. 2b), the prognoses of patients who received adjuvant chemotherapies were better than those who did not receive such treatment, with reference to each risk factor. In particular, in the two-risk-factor group the survival of those who received adjuvant chemotherapy was significantly better than that of those who did not receive chemotherapy (Fig. 2c).

Figure 3 shows the RFS curves by the SUV_{max} in adenocarcinoma (Fig. 3a) and non-adenocarcinoma patients (Fig. 3b), and by LNRs in adenocarcinoma (Fig. 3c) and non-adenocarcinoma patients (Fig. 3d). Regardless of the histology, patients with an SUV_{max} higher than 6.5 or LNRs over 0.12 had poorer prognoses than those without such values.

Discussion

In the present study, both the SUV_{max} of the primary tumor via ^{18}F-FDG-PET and the LNR were shown to be independent prognostic factors of the RFS in NSCLC patients with lymph node metastases (thus of the pathological N1 and N2). However, only the SUV_{max} was a good predictor of tumor recurrence in node-positive NSCLC patients.

^{18}F-FDG-PET is useful in various forms of lung cancer assessment, including the clinical diagnosis, evaluation of the pre-treatment extent of lymph node and distant metastasis, post-treatment assessment of the metabolic response, and determination of therapeutic effects after chemotherapy or radiotherapy [26, 27]. The intensity of the ^{18}F-FDG accumulation by the main tumor reflects the metabolic activity thereof. Previous studies have shown that ^{18}F-FDG-PET data and the tumor SUV_{max} are useful to predict recurrence in and the prognosis of NSCLC patients with stage IA [9], stage I [8, 28], and stage I or II [29, 30] disease, or T1 adenocarcinoma [11]. Okereke et al. showed that the SUV_{max} was predictive of the survival, particularly in patients with no mediastinal lymph node metastasis [10]. A systematic review and a meta-analysis by the

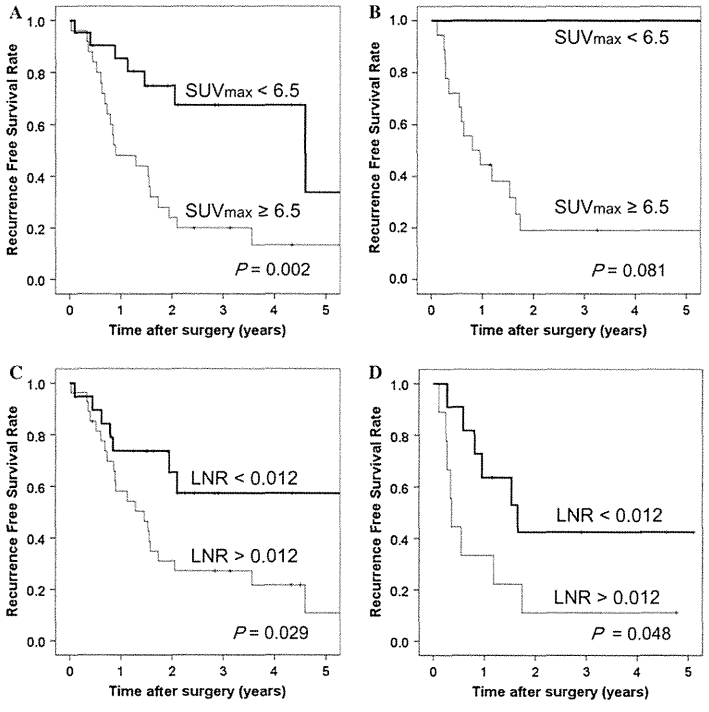

Fig. 3 Recurrence-free survival curves stratified by the cut-off values of the SUV_{max} in adenocarcinoma (**a**) and non-adenocarcinoma (**b**) patients, and the cut-off values of the LNR in adenocarcinoma (**c**) and non-adenocarcinoma patients (**d**). Regardless of tumor histology, patients with an SUV_{max} higher than 6.5 and LNRs higher than 0.12 had poorer prognoses than those who did not

European Lung Cancer Working Party showed that the SUV_{max} was a prognostic value in 13 studies on NSCLC [31]. The SUV increases when the tumor diameter becomes greater or when the cancer is at an advanced stage [10, 32]. Therefore, we examined the prognostic significance of the SUV_{max} in pathological node-positive NSCLC patients. In practical terms, the SUV_{max} was correlated with the pathological T factor, however, the SUV_{max} was also shown to be an independent prognostic factor, whereas the pathological T factor was not. Our study thus suggests that the SUV_{max} of the main tumor could be the most valuable surrogate marker of tumor aggressiveness and cancer recurrence in NSCLC patients with lymph node metastases. ^{18}F-FDG-PET findings on primary tumors have been reported to predict both the survival and local control in NSCLC patients treated with radiotherapy [33, 34] and chemoradiotherapy [35, 36]. This suggests that ^{18}F-FDG-PET is also useful for evaluating the prognoses of patients with locally advanced lung cancer, regardless of treatment modality.

The LNR has also been reported to be a good predictor of recurrence and the survival after complete resection of NSCLC [13–16, 22, 37–39]. Qiu et al. reported that the LNR was a valuable prognostic marker, particularly in patients with pathological N1 disease [14]. Some reports have shown that the LNR was a significant prognostic factor in N1 NSCLC patients [16, 22, 37], and others showed that this was also the case in both N1 and N2 patients, or in one or the other group [13, 15, 38, 39]. The cut-off LNR values differed among reports, ranging from 0.12 (12 %) to 0.35 (35 %). Therefore, the "true" cut-off value must be validated in a large cohort of N1 and N2 patients, evaluated both individually and in combination, and the significance thereof compared with that of N descriptors of the TNM classification. As the LNR is affected by the number of dissected and examined lymph nodes [39], a low cut-off value could assure the trustworthiness of lymph node dissection and could also be applied in our present study. We found that the LNR was closely associated with both the pathological nodal stage of the TNM classification and lymphatic permeation. The LNR may also be an optimal simple surrogate marker of lymphatic expansion in NSCLC patients with lymph node metastases.

In the present study, we showed that adjuvant chemotherapy was a significant favorable prognostic factor in terms

of the RFS, and, especially, such therapy was more effective in high-risk patients with node-positive NSCLC who had a high SUV_{max} and elevated LNRs. The tumor SUV_{max} has also been reported to be a good indicator of the need for adjuvant chemotherapy in patients with pathological T1b-2aN0M0 lung adenocarcinoma [40]. Wang et al. reported that the survival rate of a high-LNR group was improved by adjuvant chemotherapy, but that of a low-LNR group was not [38]. Urban et al. reported that only N2 patients with LNRs over 50 % showed survival benefits by postoperative radiotherapy. These findings support the idea that higher SUV_{max} and LNRs indicate a further need for adjuvant treatment. Although the survival benefit of adjuvant chemotherapy might be affected by selection bias, prognostic differences in the performance status (PS) and age and correlations between the SUV_{max}, LNRs and PS, age were not significant.

The SUV_{max} is known to vary by tumor histology, and the SUV_{max} of squamous cell carcinoma is higher than that of adenocarcinoma [41]. The SUV_{max} was also associated with the histological findings in the present study, and we therefore explored whether the cut-off value for all patients was the same as the values for both adenocarcinoma and non-adenocarcinoma patients. In non-adenocarcinoma patients, the small sample size ($N = 20$) indicated that only a tendency toward an influence on the survival was evident; however, in adenocarcinoma patients, a significant survival difference was evident between the high and low SUV_{max} groups.

There are some limitations associated with the present study, including the small sample size and the short follow-up duration. It may have been better to investigate the patient prognoses after stratification into the N classes N1 and N2. However, in this study, the LNR had a stronger prognostic impact than the nodal status. We were able to define a suitable LNR cut-off value for our present patient cohort. We explored the RFS and RFP in terms of the survival, because of the risk of nodal disease recurrence, however, no significant between-group survival differences were observed when it was sought to use variables, including LNR and SUV_{max}, to predict the OS.

Conclusions

In conclusion, both the SUV_{max} and the LNR serve as prognostic factors for patients with resected pathologically node-positive NSCLC. The combination of the SUV_{max} (a clinical factor) and the LNR (a pathological factor) is potentially useful to predict the prognoses of NSCLC patients with pathological nodal disease. Further validation is required to determine the appropriate cut-off values and to clarify whether the LNR or nodal status better predicts the prognosis.

Acknowledgments The support of data collection by Ms. Kaori Takeshita is gratefully acknowledged.

Compliance with ethical standards

Conflict of interest All authors participated in this study and agreed on the content of this paper. None of them have any financial or other relations that could lead to a conflict of interest.

References

1. Asamura H, Goya T, Koshiishi Y, Sohara Y, Eguchi K, Mori M, Nakanishi Y, Tsuchiya R, Shimokata K, Inoue H, Nukiwa T, Miyaoka E. A Japanese lung cancer registry study: prognosis of 13,010 resected lung cancers. J Thorac Oncol. 2008;3:46–52.
2. Li L, Ren S, Zhang Y, Guan Y, Zhao J, Liu J, Wang Q, Chen G, Chen H, Xiang J, Fu X. Risk factors for predicting the occult nodal metastasis in T1-2N0M0 NSCLC patients staged by PET/CT: potential value in the clinic. Lung Cancer. 2013;81:213–7.
3. Miyasaka Y, Suzuki K, Takamochi K, Matsunaga T, Oh S. The maximum standardized uptake value of fluorodeoxyglucose positron emission tomography of the primary tumour is a good predictor of pathological nodal involvement in clinical N0 non-small-cell lung cancer. Eur J Cardiothorac Surg. 2013;44:83–7.
4. Casiraghi M, Travaini LL, Maisonneuve P, Tessitore A, Brambilla D, Agoglia BG, Guarize J, Spaggiari L. Lymph node involvement in T1 non-small-cell lung cancer: could glucose uptake and maximal diameter be predictive criteria? Eur J Cardiothorac Surg. 2011;39:e38–43.
5. Perigaud C, Bridji B, Roussel JC, Sagan C, Mugniot A, Duveau D, Baron O, Despins P. Prospective preoperative mediastinal lymph node staging by integrated positron emission tomography-computerised tomography in patients with non-small-cell lung cancer. Eur J Cardiothorac Surg. 2009;36:731–6.
6. Bille A, Pelosi E, Skanjeti A, Arena V, Errico L, Borasio P, Mancini M, Ardissone F. Preoperative intrathoracic lymph node staging in patients with non-small-cell lung cancer: accuracy of integrated positron emission tomography and computed tomography. Eur J Cardiothorac Surg. 2009;36:440–5.
7. Imai K, Minamiya Y, Saito H, Motoyama S, Sato Y, Ito A, Yoshino K, Kudo S, Takashima S, Kawaharada Y, Kurihara N, Orino K, Ogawa J. Diagnostic imaging in the preoperative management of lung cancer. Surg Today. 2014;44:1197–206.
8. Shiono S, Abiko M, Sato T. Positron emission tomography/computed tomography and lymphovascular invasion predict recurrence in stage I lung cancers. J Thorac Oncol. 2011;6:43–7.
9. Tsutani Y, Miyata Y, Nakayama H, Okumura S, Adachi S, Yoshimura M, Okada M. Prediction of pathologic node-negative clinical stage IA lung adenocarcinoma for optimal candidates undergoing sublobar resection. J Thorac Cardiovasc Surg. 2012;144:1365–71.
10. Okereke IC, Gangadharan SP, Kent MS, Nicotera SP, Shen C, DeCamp MM. Standard uptake value predicts survival in non-small cell lung cancer. Ann Thorac Surg. 2009;88:911–5 **discussion 915–916**.
11. Higashi K, Sakuma T, Ito K, Niho S, Ueda Y, Kobayashi T, Sekiguchi R, Takahashi T, Kato T, Tonami H. Combined evaluation of preoperative FDG uptake on PET, ground-glass opacity area on CT, and serum CEA level: identification of both low and high risk of recurrence in patients with resected T1 lung adenocarcinoma. Eur J Nucl Med Mol Imaging. 2009;36:373–81.
12. Fukumoto K, Taniguchi T, Usami N, Kawaguchi K, Fukui T, Ishiguro F, Nakamura S, Yokoi K. Preoperative plasma D-dimer level

is an independent prognostic factor in patients with completely resected non-small cell lung cancer. Surg Today. 2015;45:63–7.
13. Taylor MD, Lapar DJ, Thomas CJ, Persinger M, Stelow EB, Kozower BD, Lau CL, Jones DR. Lymph node ratio predicts recurrence and survival after R0 resection for non-small cell lung cancer. Ann Thorac Surg. 2013;96:1163–70.
14. Qiu C, Dong W, Su B, Liu Q, Du J. The prognostic value of ratio-based lymph node staging in resected non-small-cell lung cancer. J Thorac Oncol. 2013;8:429–35.
15. Matsuguma H, Oki I, Nakahara R, Ohata N, Igarashi S, Mori K, Endo S, Yokoi K. Proposal of new nodal classifications for non-small-cell lung cancer based on the number and ratio of metastatic lymph nodes. Eur J Cardiothorac Surg. 2012;41:19–24.
16. Jonnalagadda S, Arcinega J, Smith C, Wisnivesky JP. Validation of the lymph node ratio as a prognostic factor in patients with N1 nonsmall cell lung cancer. Cancer. 2011;117:4724–31.
17. Li X, Zhang H, Xing L, Ma H, Xie P, Zhang L, Xu X, Yue J, Sun X, Hu X, Chen M, Xu W, Chen L, Yu J. Mediastinal lymph nodes staging by ^{18}F-FDG PET/CT for early stage non-small cell lung cancer: a multicenter study. Radiother Oncol. 2012;102:246–50.
18. Hellwig D, Graeter TP, Ukena D, Groeschel A, Sybrecht GW, Schaefers HJ, Kirsch CM. 18F-FDG PET for mediastinal staging of lung cancer: which SUV threshold makes sense? J Nucl Med. 2007;48:1761–6.
19. Sanli M, Isik AF, Zincirkeser S, Elbek O, Mete A, Tuncozgur B, Elbeyli L. Reliability of positron emission tomography-computed tomography in identification of mediastinal lymph node status in patients with non-small cell lung cancer. J Thorac Cardiovasc Surg. 2009;138:1200–5.
20. Ohtaki Y, Shimizu K, Kakegawa S, Nagashima T, Nakano T, Atsumi J, Enokida Y, Igai H, Ibe T, Sugano M, Kamiyoshihara M, Kawashima O, Kaira K, Sunaga N, Takeyoshi I. Postrecurrence survival of surgically resected pulmonary adenocarcinoma patients according to and mutation status. Mol Clin Oncol. 2014;2:187–96.
21. Ludwig MS, Goodman M, Miller DL, Johnstone PA. Postoperative survival and the number of lymph nodes sampled during resection of node-negative non-small cell lung cancer. Chest. 2005;128:1545–50.
22. Li ZM, Ding ZP, Luo QQ, Wu CX, Liao ML, Zhen Y, Chen ZW, Lu S. Prognostic significance of the extent of lymph node involvement in stage II-N1 non-small cell lung cancer. Chest. 2013;144:1253–60.
23. Miyamae Y, Shimizu K, Mitani Y, Araki T, Kawai Y, Baba M, Kakegawa S, Sugano M, Kaira K, Lezhava A, Hayashizaki Y, Yamamoto K, Takeyoshi I. Mutation detection of epidermal growth factor receptor and KRAS genes using the smart amplification process version 2 from formalin-fixed, paraffin-embedded lung cancer tissue. J Mol Diagn. 2010;12:257–64.
24. Kakegawa S, Shimizu K, Sugano M, Miyamae Y, Kaira K, Araki T, Nakano T, Kamiyoshihara M, Kawashima O, Takeyoshi I. Clinicopathological features of lung adenocarcinoma with KRAS mutations. Cancer. 2011;117:4257–66.
25. Araki T, Shimizu K, Nakamura K, Nakamura T, Mitani Y, Obayashi K, Fujita Y, Kakegawa S, Miyamae Y, Kaira K, Ishidao T, Lezhava A, Hayashizaki Y, Takeyoshi I, Yamamoto K. Usefulness of peptide nucleic acid (PNA)-clamp smart amplification process version 2 (SmartAmp2) for clinical diagnosis of KRAS codon 12 mutations in lung adenocarcinoma: comparison of PNA-clamp SmartAmp2 and PCR-related methods. J Mol Diagn. 2010;12:118–24.
26. van Elmpt W, Ollers M, Dingemans AM, Lambin P, De Ruysscher D. Response assessment using 18F-FDG PET early in the course of radiotherapy correlates with survival in advanced-stage non-small cell lung cancer. J Nucl Med. 2012;53:1514–20.
27. Jeong JU, Chung WK, Nam TK, Song JY, Yoon MS, Kim YC, Kim KS, Oh IJ, Ban HJ, Kwon SY, Bom HS, Ahn SJ. Early metabolic response on 18F-fluorodeoxyglucose-positron-emission tomography/computed tomography after concurrent chemoradiotherapy for advanced stage III non-small cell lung cancer is correlated with local tumor control and survival. Anticancer Res. 2014;34:2517–23.
28. Higashi K, Ueda Y, Arisaka Y, Sakuma T, Nambu Y, Oguchi M, Seki H, Taki S, Tonami H, Yamamoto I. 18F-FDG uptake as a biologic prognostic factor for recurrence in patients with surgically resected non-small cell lung cancer. J Nucl Med. 2002;43:39–45.
29. Koo HK, Jin SM, Lee CH, Lim HJ, Yim JJ, Kim YT, Yang SC, Yoo CG, Han SK, Kim JH, Shim YS, Kim YW. Factors associated with recurrence in patients with curatively resected stage I–II lung cancer. Lung Cancer. 2011;73:222–9.
30. Agarwal M, Brahmanday G, Bajaj SK, Ravikrishnan KP, Wong CY. Revisiting the prognostic value of preoperative (18) F-fluoro-2-deoxyglucose ((18)F-FDG) positron emission tomography (PET) in early-stage (I & II) non-small cell lung cancers (NSCLC). Eur J Nucl Med Mol Imaging. 2010;37:691–8.
31. Berghmans T, Dusart M, Paesmans M, Hossein-Foucher C, Buvat I, Castaigne C, Scherpereel A, Mascaux C, Moreau M, Roelandts M, Alard S, Meert AP, Patz EF Jr, Lafitte JJ, Sculier JP. Primary tumor standardized uptake value (SUVmax) measured on fluorodeoxyglucose positron emission tomography (FDG-PET) is of prognostic value for survival in non-small cell lung cancer (NSCLC): a systematic review and meta-analysis (MA) by the European Lung Cancer Working Party for the IASLC Lung Cancer Staging Project. J Thorac Oncol. 2008;3:6–12.
32. Cerfolio RJ, Bryant AS, Ohja B, Bartolucci AA. The maximum standardized uptake values on positron emission tomography of a non-small cell lung cancer predict stage, recurrence, and survival. J Thorac Cardiovasc Surg. 2005;130:151–9.
33. Na F, Wang J, Li C, Deng L, Xue J, Lu Y. Primary tumor standardized uptake value measured on F18-Fluorodeoxyglucose positron emission tomography is of prediction value for survival and local control in non-small-cell lung cancer receiving radiotherapy: meta-analysis. J Thorac Oncol. 2014;9:834–42.
34. Ulger S, Demirci NY, Eroglu FN, Cengiz HH, Tunc M, Tatci E, Yilmaz U, Cetin E, Avci E, Cengiz M. High FDG uptake predicts poorer survival in locally advanced nonsmall cell lung cancer patients undergoing curative radiotherapy, independently of tumor size. J Cancer Res Clin Oncol. 2014;140:495–502.
35. Cook GJ, Yip C, Siddique M, Goh V, Chicklore S, Roy A, Marsden P, Ahmad S, Landau D. Are pretreatment ^{18}F-FDG PET tumor textural features in non-small cell lung cancer associated with response and survival after chemoradiotherapy? J Nucl Med. 2013;54:19–26.
36. Lee VH, Chan WW, Lee EY, Choy TS, Ho PP, Leung DK, Lam KO, Kwong DL, Leung TW, Khong PL. Prognostic significance of standardized uptake value of lymph nodes on survival for stage III non-small cell lung cancer treated with definitive Concurrent chemoradiotherapy. Am J Clin Oncol. 2014 **[Epub ahead of print]**.
37. Wisnivesky JP, Arciniega J, Mhango G, Mandeli J, Halm EA. Lymph node ratio as a prognostic factor in elderly patients with pathological N1 non-small cell lung cancer. Thorax. 2011;66:287–93.
38. Wang CL, Li Y, Yue DS, Zhang LM, Zhang ZF, Sun BS. Value of the metastatic lymph node ratio for predicting the prognosis of non-small-cell lung cancer patients. World J Surg. 2012;36:455–62.
39. Urban D, Bar J, Solomon B, Ball D. Lymph node ratio may predict the benefit of postoperative radiotherapy in non-small-cell lung cancer. J Thorac Oncol. 2013;8:940–6.

40. Sasada S, Miyata Y, Tsubokawa N, Mimae T, Yoshiya T, Okada M. Role of positron emission tomography/computed tomography findings for adjuvant chemotherapy indications in stage T1b-2aN0M0 lung adenocarcinoma. Ann Thorac Surg. 2014;98:417–22.

41. Al-Sarraf N, Gately K, Lucey J, Aziz R, Doddakula K, Wilson L, McGovern E, Young V. Clinical implication and prognostic significance of standardised uptake value of primary non-small cell lung cancer on positron emission tomography: analysis of 176 cases. Eur J Cardiothorac Surg. 2008;34:892–7.

Breast Cancer
DOI 10.1007/s12282-015-0641-8

ORIGINAL ARTICLE

APOBEC3B high expression status is associated with aggressive phenotype in Japanese breast cancers

Miki Tsuboi[1,2] · Arito Yamane[2] · Jun Horiguchi[1] · Takehiko Yokobori[2] · Reika Kawabata-Iwakawa[3] · Shinji Yoshiyama[3] · Susumu Rokudai[2] · Hiroki Odawara[5] · Hideaki Tokiniwa[1] · Tetsunari Oyama[4] · Izumi Takeyoshi[1] · Masahiko Nishiyama[2]

Received: 31 March 2015 / Accepted: 18 September 2015

Abstract
Background The members of AID/APOBEC protein family possess cytidine deaminase activity that converts cytidine residue to uridine on DNA and RNA. Recent studies have shown the possible influence of *APOBEC3B* (*A3B*) as DNA mutators of breast cancer genome. However, the clinical significance of *A3B* expression in Japanese breast cancer has not been studied in detail.
Methods Ninety-three primary breast cancer tissues (74 estrogen-receptor (ER) positive, 3 ER and HER2 positive, 6 HER2 positive, and 10 triple negative) including 37 tumor-normal pairs were assessed for *A3B* mRNA expression using quantitative real-time RT-PCR. We analyzed the relation between *A3B* expression, mutation analysis of *TP53* and *PIK3CA* by direct sequencing, polymorphic *A3B* deletion allele and human papillomavirus (HPV) infection in tumors.
Results *A3B* mRNA was overexpressed in tumors compared with normal tissue. Patients with high *A3B* expression were associated with subtype and progression of lymph node metastasis and pathological nuclear grade. However, the expression was not related to any other clinicopathological factors, including mutation of *TP53* and *PIK3CA*, polymorphic *A3B* deletion allele, HPV infection and survival time.
Conclusion The expression of *A3B* in breast cancer was higher than in non-cancerous tissues and was related to the lymph node metastasis and nuclear grade, which are reliable aggressive phenotype markers in breast cancer. Evaluation of *A3B* expression in tumor may be a marker for breast cancer with malignant potential.

Keywords Breast cancer · APOBEC3B · Nuclear grade

Introduction

Tens of thousands of genomic mutations have been observed in human cancers, and several mutations are prerequisites for carcinogenesis. These mutations promote clonal diversities among cancer cells, and clinically they also promote metastasis and resistance to therapy [1]. Base substitutions are the most frequent mode of mutations, and some of them can be induced by DNA damage from extrinsic carcinogens and erroneous DNA repair machineries [2]. For most base substitutions, however, the specific mechanism that introduces them to the cellular genome remains unclear.

Recent genome-wide analysis of the mutation pattern of breast cancers confirmed the domination of C to T

Electronic supplementary material The online version of this article (doi:10.1007/s12282-015-0641-8) contains supplementary material, which is available to authorized users.

✉ Masahiko Nishiyama
m.nishiyama@gunma-u.ac.jp

[1] Department of Thoracic Visceral Organ Surgery, Gunma University Graduate School of Medicine, 3-39-22 Showa-machi, Maebashi, Gunma 371-8511, Japan

[2] Department of Molecular Pharmacology and Oncology, Gunma University Graduate School of Medicine, 3-39-22 Showa-machi, Maebashi, Gunma 371-8511, Japan

[3] Initiative for Advanced Research, Gunma University, 3-39-22 Showa-machi, Maebashi, Gunma 371-8511, Japan

[4] Diagnostic Pathology, Gunma University Graduate School of Medicine, 3-39-22 Showa-machi, Maebashi, Gunma 371-8511, Japan

[5] Department of Surgery, Toho Hospital, 1155 Azami, Kasakake-machi, Midorishi, Gunma 379-2311, Japan

Published online: 17 October 2015

transitions with a strong bias toward 5′-TCA-3′ context [3]. A nuclear localizing cytidine deaminase, *APOBEC3B* (*A3B*), which shows the sequence preference of TCA signature in vitro, has been identified as a possible contributor to the C to T transitions in breast cancer genome: It works as the mutational source on genomic DNA of many types of cancers including breast cancers [4].

In one cohort in the U.S., high expression of *A3B* mRNA has been observed in about half of breast cancers [4]. The authors have also showed in cultured breast cancer cells that A3B has mutational induction activity on *TP53* gene [4]. *A3B* expression has been also reported to be induced transcriptionally by the human papillomavirus (HPV) 16 infection [5]. Breast cancers with high *A3B* mRNA expression harbor more mutations in genome and show poorer post-operative disease-free survival (DFS) among ER-positive, lymph node negative breast cancers without adjuvant therapy [6]. This observation suggests that the mutational function of *A3B* may contribute to breast cancer carcinogenesis and/or have prognostic significance among breast cancers.

In some reports, breast cancers in Asia including Japan have shown some clinical differences from Western countries in terms of incidence [7] and outcomes [8]. Those clinical differences might be, at least in part, attributed to genetic differences among ethnicities [9]. A common polymorphism of *APOBEC3s* gene clustered on 22q13 deletes 29.5 kb region including the entire *A3B* coding region, leaving only 3′-UTR. The prevalence of the polymorphic deletion allele greatly differs among groups: Higher incidence (40–90 %) of deletion allele has been reported in East Asian and Pacific Islander populations than in African and European populations (0.9–6 %) [10, 11]. On the other hand, an intriguing observation on the deletion polymorphism and genome-wide mutations has reported that the deletion alleles are found to be a risk allele for incidence of breast cancer [12]. They have higher content of *APOBEC* mutation signature even without *A3B* coding regions [2, 13]. It is still under debate how the *A3B* deletion allele contributes to breast cancer mutations. However, the wide variations in prevalence of *A3B* deletion allele among various populations strongly suggests different influences of *A3B* in breast cancer carcinogenesis, development, and prognosis among the population groups.

The purpose of this research is to clarify the clinical significance of *A3B* expression in Japanese breast cancer patients. Therefore, we examined *A3B* mRNA expression in primary breast cancer in a Japanese cohort. We also analyzed the association between *A3B* expression, *A3B* insertion/deletion allele, mutation status of *TP53* and *PIK3CA*, HPV infection, clinicopathological characteristics and clinical outcome.

Materials and methods

Patient samples

Ninety-three patients who underwent surgical excision of breast cancer at Gunma University Hospital between 2007 and 2012 were involved in the study. Tumor samples were immediately frozen after surgery and stored at −80 °C until DNA and RNA isolation. The study was approved by Ethics Committee for Human Genome Research of Gunma University Graduate School of Medicine (protocol number 182) and patients provided written informed consent.

RT-qPCR assay for *APOBEC3B* gene

Total RNA was extracted from breast cancer and adjacent normal breast tissues using NucleoSpin RNA II kit (Macherey–Nagel) with Mixer Mill MM300 (Retsch) according to the manufacturer's instructions. RNA concentration was determined by a Thermo Scientific™ NanoDrop Lite. One μg of total RNA was then used for synthesis of cDNA using a ReverTra Ace qPCR RT Kit (Toyobo, Osaka, Japan) according to the manufacturer's recommendations. One μl of each reverse transcript reaction was used for PCR analysis. The *A3B* qPCR assay reactions were performed using KAPA PROBE FAST qPCR Kits (Kapa Biosystems) in a 20-μl reaction volume on StepOnePlus™ Systems (Life Technologies) with a VIC probe for ACTB gene (Life Technologies, 4326315E) as internal control. The primers and a probe used for the *A3B* gene were: forward, 5-CGCCAGACCTACTTGTGC TA-3 and the reverse, 5-GCCACAGAGAAGATTCTTAG CC-3 (111 bp), Universal Probe Library #39 (Roche). The cycling conditions used were: initial denaturation at 95 °C for 3 min, followed by 40 cycles at 95 °C for 3 s and 60 °C for 20 s.

Mutation status of *TP53* and *PIK3CA* genes

PCR reactions using cDNA were performed using Kapa HiFi HotStart ReadyMix PCR Kit (Kapa Biosystems) in a 25-μl reaction volume with an initial denaturation step at 95 °C for 3 min, followed by 30 cycles of 98 °C 20 s, 60 °C 15 s, and 72 °C at 1 min. The final extension step was at 72 °C for 1 min. Mutation hotspots in exon 2–11 of *TP53* and exon 9/20 of *PIK3CA* were assessed by direct sequencing of the PCR products. Primers used were TP53fragment1-F: GACACGCTTCCCTGGATTGGC, TP53fragment1-R: GCAAAACATCTTGTTGAGGGCA, TP53fragment1-seq: CAGGGGAGTACGTGCAAGTCAC

AG, TP53fragment2-F: GTTTCCGTCTGGGCTTCTTG CA, TP53fragment2-R: GGTACAGTCAGAGCCAACCT, TP53fragment2-seq: GCCAACCTCAGGCGGCTCATA, TP53fragment3-F: TGGCCCCTCCTCAGCATCTTA, TP5 3fragment3-R: CAAGGCCTCATTCAGCTCTC, TP53 fragment3-seq: CGAGTGGAAGGAAATTTGCGT, TP53 fragment4-F: CGGCGCACAGAGGAAGAGAATC, TP53 fragment4-R: CAAGGCCTCATTCAGCTCTC, TP53 fragment4-seq: GGGGAGCCTCACCACGAGCTG, PIK 3CA_ex9-F: TGGCCAGTACCTCATGGATTAGAA, PIK3CA_exon9-R: GAGGCCAATCTTTTACCAAGCA, PIK3CA_exon9-seq: TACATCTGGGCTACTTCATCTC-TAG, PIK3CA_exon20-F: AATGCACAAAGACAAGAG AATTTGAG, PIK3CA_exon20-R: AATTCCTATGCAAT CGGTCTTTGC, PIK3CA_ex20-seq: GCAGTGTGGAAT CCAGAGTGAG.

DNA extraction and PCR with HPV 16-specific primers

Among 93 breast cancer samples in which *A3B* mRNA levels were measured, HPV16 infection was examined in 88 genomic DNA samples from the available frozen breast cancer tissue. DNA extraction was performed using NucleoSpin Tissue kit (Takara bio, Japan) according to the manufacturer's protocol. PCR reaction using DNA were performed using Kapa HiFi HotStart ReadyMix PCR Kit (Kapa Biosystems) in a 25-μl reaction volume with an initial denaturation step at 95 °C for 3 min, followed by 40 cycles of 98 °C 20 s, 60 °C 15 s, and 72 °C at 1 min, and a final extension step at 72 °C for 1 min. Primers used were HPV16-F; AGGGCGTAACCGAAATCGGT: HPV16-R: CTGAGCTGTCATTTAATTGCTCA. The final PCR product of 10 μl was loaded onto 1 % agarose gel, stained with ethidium bromide, and visualized under UV illumination.

DNA extraction and PCR genotyping assay of *A3B* deletion

Among 93 breast cancer samples in which *A3B* mRNA levels were measured, *A3B* deletion allele was examined in 32 genomic DNA samples from available adjacent normal breast tissue. DNA extraction was performed using NucleoSpin Tissue kit (Takara bio, Japan) according to the manufacturer's protocol. We performed PCR using oligonucleotide sequences as described previously [10, 14]: Deletion_F; TAGGTGCCACCCCGAT: Deletion_R; TTGAGCATAATCTTACTCTTGTAC (700 bp): Insertion1_F; TGTCCCTTTTCAGAGTTTGAGTA: Insertion1_R; TGGAGCCAATTAATCACTTCAT (705 bp) [10]: Insertion2_F; GAGTGGAAGCGCCTCCTC: Insertion2_R; CTCCTGGCCAGCCTAGC (811 bp) [14].

Insertion and deletion PCR assays were performed separately. The final PCR product of 10 μl was loaded onto 1 % agarose gel, stained with ethidium bromide, and visualized under UV illumination.

PCR reactions using DNA (50 ng) were performed using Phusion High-Fidelity DNA Polymerase (New England Biolabs Japan) in a 50-μl reaction volume with an initial denaturation step at 98 °C for 5 min, followed by 30

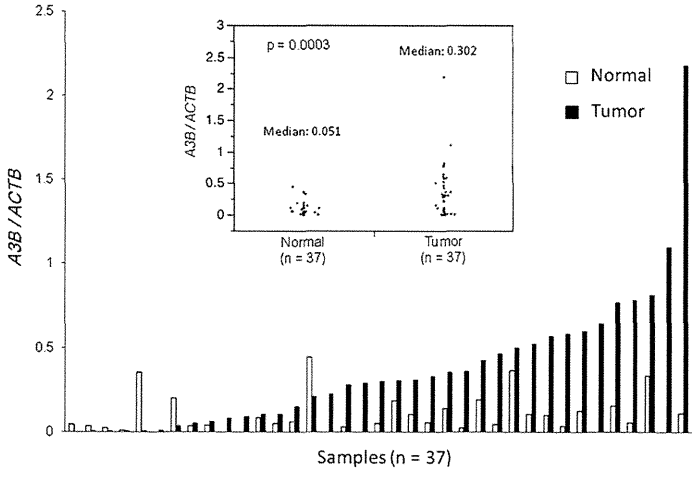

Fig. 1 *A3B* expression in breast tumors and adjacent normal breast tissues. *A3B* mRNA expression relative to *ACTB* in 37 breast cancer tissue samples and paired with adjacent normal breast tissues. *A3B* expression level is significantly higher in tumor tissue compared with normal tissue (Mann–Whitney test, $p = 0.003$)

Table 1 Patient characteristics and *A3B* mRNA expression level

Characteristics	*A3B* relative expression		*p* value
	Low expression $n = 63$	High expression $n = 30$	
Age (years)	57.9 ± 13.1	54.9 ± 11.6	0.29
Menopausal status			0.52
Premenopausal	25	14	
Postmenopausal	38	16	
Subtype			0.034*
ER (+)	54	20	
ER (+)/HER2 (+)	0	3	
HER2 (+)	4	2	
Triple negative	5	5	
PgR			0.64
−	18	10	
+	45	20	
Deletion allele (n=32)			0.0019*
Insertion/insertion	1	10	
Deletion/insertion	14	7	
Stage			0.66
0	1	0	
I	21	7	
II	35	20	
III	6	3	
Lymph node metastasis			0.033*
−	40	12	
+	23	18	
Lymphatic invasion			0.079**
−	19	4	
+	44	26	
Venous invasion			0.066**
−	51	19	
+	12	11	
Nuclear grade			0.009*
NG1	17	2	
NG2	24	8	
NG3	22	20	

* $p < 0.05$; ** $p < 0.1$

cycles of 98 °C 10 s, 50 °C 30 s, and 72 °C at 10 s, and a final extension step at 72 °C for 3 min.

Statistical analysis

Statistical significance was estimated using Student's *t* test, Mann–Whitney test, ANOVA, and Chi-square test. Kaplan–Meier curves were generated for overall survival (OS) and DFS, and statistical significance was determined using the log-rank test. A probability value of <0.05 was considered significant. All statistical analyses were performed using JMP software (SAS Institute Inc.).

Results

A3B mRNA is expressed in tumor tissues of Japanese breast cancer patients

First, to determine whether *A3B* was highly expressed in Japanese breast cancers, we quantified *A3B* mRNA expression by RT-qPCR from fresh frozen tumor samples. Thirty-seven paired adjacent normal breast tissue samples were also available for *A3B* quantification (Supplementary Table 1). *A3B/ACTB* mRNA levels (median 0.302) in the breast cancer tissues were significantly higher than in the

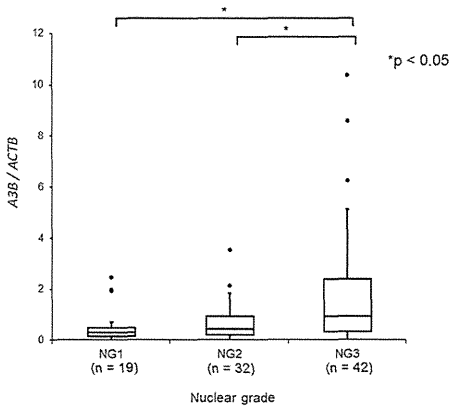

Fig. 2 *A3B* mRNA expression level correlates with pathological nuclear glade. Relative expression levels of *A3B* mRNA are plotted in each pathological nuclear grade group. *Box plot* shows ±1SD. *Asterisk* denotes $p < 0.05$

adjacent normal breast tissues (median 0.051) ($p = 0.0003$) (Fig. 1). Approximately half of the tumor tissues showed higher *A3B* mRNA expression than did the adjacent normal tissues.

The clinical significance of A3B expression in breast cancer patients

We divided 93 breast cancer patients into two groups according to the levels of *A3B* expression in tumor tissues. The cut off point was the mean expression level of *A3B* in tumor (high expression group, $n = 30$; low expression group, $n = 63$). Clinicopathological factors were significantly different in the *A3B* high expression group. *A3B* high expression correlated with the breast cancer subtype ($p = 0.034$) and progression of lymph node metastasis ($p = 0.033$), lymphatic invasion ($p = 0.079$), venous invasion ($p = 0.066$), and pathological nuclear grade ($p = 0.009$) (Table 1; Fig. 2), compared with the *A3B* low expression group. Moreover, *A3B* expression in cases with *A3B* deletion allele was significantly lower than that of cases with *A3B* insertion allele ($p = 0.0019$) (Table 1). No significant differences were observed regarding age, menopausal status, PgR status, or clinical stage (Table 1). The status of polymorphic *A3B* deletion allele in 32 breast cancer patients was not significantly associated with clinicopathological factors (Table 2; Supplementary Fig. 1).

A3B mRNA expression levels were not predictors of clinical outcome among Japanese breast cancer patients

To determine whether *A3B* mRNA expression was associated with clinical outcome in our Japanese cohort, we compared DFS and OS in the high and low *A3B* expression groups. As a result, we did not find significant differences in DFS and OS among any patients or in the ER-positive group (Fig. 3). Among patients with no lymph node metastasis, patients with high *A3B* expression were not associated with DFS or OS (Supplementary Fig. 2).

TP53/PIK3CA driver mutations and HPV infection were not associated with A3B expression in breast cancers in this study

We performed PCR-direct sequence of *TP53* and *PIK3CA* mutational hotspots from cDNA to determine whether the level of *A3B* mRNA expression was associated with *TP53* and *PIK3CA* driver gene mutation status. *TP53* mutation at exon 2–11 and *PIK3CA* mutations at exon 9 and exon 20 hotspots were found in 16.7 and 15.7 %, respectively in of the samples. No correlation was found between *A3B* expression and *TP53/PIK3CA* mutation status in our cohort (Fig. 4a, b). HPV16 infection, known as an *A3B*-inducer, was detected in 27.3 % (24/88) of patients in our cohort, but the infection was not significantly associated with *A3B* expression (Fig. 4c).

Discussion

In the present study, we found that expression levels of *A3B* mRNA in breast cancer tissue were significantly higher than in adjacent normal breast tissue of Japanese patients. Moreover, breast cancer patients with high *A3B* expression were associated with breast cancer subtype, progression of lymph node metastasis and pathological nuclear grade. However, the expression was not related to the other clinicopathological factors, i.e. mutation of *TP53* and *PIK3CA*, status of polymorphic *A3B* deletion allele, HPV16 infection and survival time.

The *A3B* was previously reported overexpressed in breast tumoral tissue compared to the normal counterpart [3]. In Western populations, prognostic significance of *A3B* expression in ER-positive lymph node-negative patients without adjuvant therapy had previously been reported [5]. The Japanese cohort in this study showed no difference in terms of DFS and OS, even though the overexpression of *A3B* observed was the same as in Western countries. This difference in clinical outcomes suggests a different mode

Table 2 Relationship of *A3B* mRNA expression and patients characteristics in 32 breast cancer patients with or without *A3B* deletion allele

Characteristics	*A3B* allele		*p* value
	Insertion/insertion $n = 11$	Deletion/insertion $n = 21$	
Age (years)	56.6 ± 14.7	51.6 ± 12.2	0.34
Menopausal status			0.91
Premenopausal	6	11	
Postmenopausal	5	10	
Subtype			
ER (+)	2	18	0.06**
ER (+)/HER2 (+)	2	0	
HER2 (+)	0	3	
Triple negative	1	0	
PgR			0.95
−	2	4	
+	9	17	
Stage			0.86
I	4	6	
II	6	12	
III	1	3	
Lymph node metastasis			0.17
−	3	11	
+	2	10	
Lymphatic invasion			0.21
−	1	6	
+	10	15	
Venous invasion			0.65
−	7	15	
+	4	6	
Nuclear grade			0.57
NG1	0	2	
NG2	3	5	
NG3	8	14	

** $p < 0.1$

of action by *A3B* according to the etiology of breast cancer among different ethnic/geographical populations [10, 11]. In our study, *A3B* expression in breast cancer patients with *A3B* deletion was significantly lower than those with *A3B* insertion. Despite the limited number of samples, A3B expression levels correlated to the genotype and malignant potential of the tumor in breast cancer patients (Table 1). Our data show that *A3B* expression is possibly a marker of tumor progression (lymph node metastasis, $p = 0.033$ and nuclear grade, $p = 0.009$) (Table 1). The *A3B* expression related better to pathological findings than *A3B* genotyping (Table 2). However, this might be caused by lower patient numbers in the genotyping data. More patients will need to be involved in future studies in order to fully elucidate clinical potential of A3B genomic analysis.

APOBEC3 family is expressed in virally infected cells where it plays a significant role in host defense against virus. Therefore, it is possible that viral infection, including HPV [15] and Epstein–Barr virus [16], may play a role in the regulation of *A3B* gene expression, in at least some breast cancers. In this study, the HPV16 infection rate was not associated with the *A3B* expression (Table 1). As for the relation between viral infection and carcinogenesis, there has been a long-standing debate about the contribution of tumor-inducing viruses [17, 18]. Future elucidation of a mechanism of *A3B* regulation may become a lead in prevention and/or treatment of viral associated-breast cancers.

A3B expression levels were reported to positively correlate with levels of genomic uracil contents,

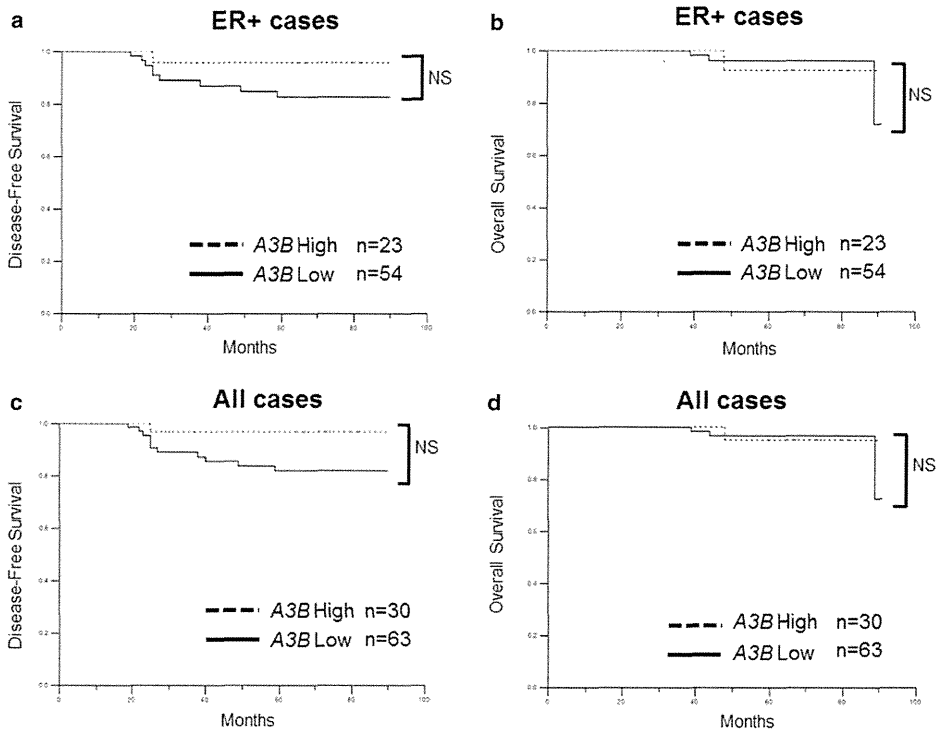

Fig. 3 Survival curves of breast cancer patients according to the level of A3B expression. Kaplan–Meier survival analysis of *A3B* expression for high and low groups in DFS (**a**) and OS (**b**) among ER-positive cases ($n = 77$) and DFS (**c**) and OS (**d**) among all cases of this cohort ($n = 93$). Cutoff value was defined as mean of *A3B* expression. *NS* not significant

frequencies of overall base substitutions, and C-to-T transitions [4]. Since *A3B* can mutate to oncogenic driver gene, deamination activity of *A3B* might contribute to breast cancer carcinogenesis. *TP53* and *PIK3CA* are the most frequently mutated genes in breast cancers [19], and tumors with *TP53* mutations are reported to have higher levels of *A3B* mRNA in TCGA and other containing Western patients databases [4]. However, *TP53* and *PIK3CA* did not show any correlation between their mutation status and *A3B* expression in our study. It has been reported that *TP53* mutation rates in triple negative breast cancer patients are higher than that in hormone receptor-positive patients [20]. Our study included only 10.8 % (10/93) triple negative breast cancer patients because of selection for patients without preoperative chemotherapies. This sample size is smaller than the one in previous report from Western countries [3]. Therefore, our mutation data might not accord with the previous studies. Although pathological nuclear grade and lymph node metastasis correlated with clinical outcomes [21], we found no correlation between *A3B* expression status and clinical stage, breast cancer subtype, prognosis or driver mutation status in our cohort. The limited number and clinical follow-up of patients in this study might have contributed to less detection power.

In conclusion, *A3B* expression could be a useful marker of aggressive breast cancer. With respect to developing new molecular cancer therapies and cancer prevention methods based on *A3B*, further studies including IHC, whole genome sequencing and larger sample numbers will be required to fully clarify the significance of *A3B* expression in Japanese breast cancer patients.

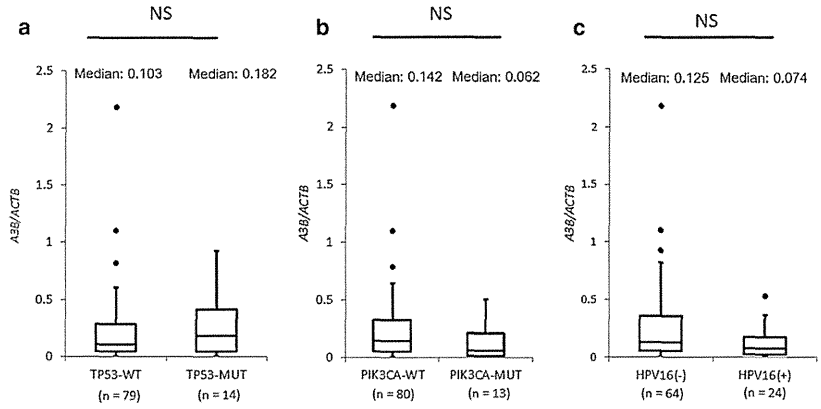

Fig. 4 *TP53/PIK3CA* mutation status, HPV 16 infection and *A3B* expression. *A3B* mRNA expression level was compared between *TP53* (**a**) and *PIK3CA* (**b**) wild-type (WT) tumors and mutated tumor (MUT) ($n = 93$). (**c**) The relation of *A3B* expression and HPV16 infection was evaluated. *NS* not significant

Acknowledgments We thank Dr. Andrei Turtoi and all members of Department of Molecular Pharmacology and Oncology and Thoracic Visceral Organ Surgery for their helpful discussions. We also thank patients who participated in this study, and Ikuko Horikoshi and Tadashi Handa for their technical assistance. The work was supported in part by Uehara Zaidan, Promotion Plan for the Platform of Human Resource Development for Cancer and New Paradigms—Establishing Centers for Fostering Medical Researchers of the Future programs by Ministry of Education, Culture, Sports, Science and Technology of Japan, and Gunma University Initiative for Advanced Research (GIAR).

Compliance with ethical standards

Conflict of interest Masahiko Nishiyama received a research grant from Yakult Honsha Co. Ltd. The other authors declare that they have no conflict of interest.

References

1. Vogelstein B, Papadopoulos N, Velculescu VE, Zhou S, Diaz LA Jr, Kinzler KW. Cancer genome landscapes. Science. 2013;339:1546–58.
2. Helleday T, Eshtad S, Nik-Zainal S. Mechanisms underlying mutational signatures in human cancers. Nat Rev Genet. 2014;15:585–98.
3. Burns MB, Lackey L, Carpenter MA, Rathore A, Land AM, Leonard B, et al. APOBEC3B is an enzymatic source of mutation in breast cancer. Nature. 2013;494:366–70.
4. Burns MB, Temiz NA, Harris RS. Evidence for APOBEC3B mutagenesis in multiple human cancers. Nat Genet. 2013;45:977–83.
5. Mori S, Takeuchi T, Ishii Y, Kukimoto I. Identification of APOBEC3B promoter elements responsible for activation by human papillomavirus type 16 E6. Biochem Biophys Res Commun. 2015;460:555–60.
6. Sieuwerts AM, Willis S, Burns MB, Look MP, Gelder ME, Schlicker A, et al. Elevated APOBEC3B correlates with poor outcomes for estrogen-receptor-positive breast cancers. Horm Cancer. 2014;5:405–13.
7. Bhoo-Pathy N, Yip CH, Hartman M, Uiterwaal CS, Devi BC, Peeters PH, et al. Breast cancer research in Asia: adopt or adapt Western knowledge? Eur J Cancer. 2013;49:703–9.
8. Maskarinec G, Sen C, Koga K, Conroy SM. Ethnic differences in breast cancer survival: status and determinants. Womens Health (Lond Engl). 2011;7:677–87.
9. Iqbal J, Ginsburg O, Rochon PA, Sun P, Narod SA. Differences in breast cancer stage at diagnosis and cancer-specific survival by race and ethnicity in the United States. JAMA. 2015;313:165–73.
10. Kidd JM, Newman TL, Tuzun E, Kaul R, Eichler EE. Population stratification of a common APOBEC gene deletion polymorphism. PLoS Genet. 2007;3:e63.
11. Komatsu A, Nagasaki K, Fujimori M, Amano J, Miki Y. Identification of novel deletion polymorphisms in breast cancer. Int J Oncol. 2008;33:261–70.
12. Long J, Delahanty RJ, Li G, Gao YT, Lu W, Cai Q, et al. A common deletion in the APOBEC3 genes and breast cancer risk. J Natl Cancer Inst. 2013;105:573–9.
13. Caval V, Suspene R, Shapira M, Vartanian JP, Wain-Hobson S. A prevalent cancer susceptibility APOBEC3A hybrid allele bearing APOBEC3B 3′UTR enhances chromosomal DNA damage. Nat Commun. 2014;5:5129.
14. Imahashi M, Izumi T, Watanabe D, Imamura J, Matsuoka K, Ode H, et al. Lack of association between intact/deletion polymorphisms of the APOBEC3B gene and HIV-1 risk. PLoS One. 2014;9:e92861.
15. Li N, Bi X, Zhang Y, Zhao P, Zheng T, Dai M. Human papillomavirus infection and sporadic breast carcinoma risk: a meta-analysis. Breast Cancer Res Treat. 2011;126:515–20.
16. Huo Q, Zhang N, Yang Q. Epstein-Barr virus infection and sporadic breast cancer risk: a meta-analysis. PLoS One. 2012;7:e31656.
17. Akhter J, Ali Aziz MA, Al Ajlan A, Tulbah A, Akhtar M. Breast cancer: is there a viral connection? Adv Anat Pathol. 2014;21:373–81.
18. Vernet-Tomas M, Mena M, Alemany L, Bravo I, De Sanjose S, Nicolau P, et al. Human papillomavirus and breast cancer: no

evidence of association in a Spanish set of cases. Anticancer Res. 2015;35:851–6.
19. Banerji S, Cibulskis K, Rangel-Escareno C, Brown KK, Carter SL, Frederick AM, et al. Sequence analysis of mutations and translocations across breast cancer subtypes. Nature. 2012;486:405–9.
20. Bertheau P, Lehmann-Che J, Varna M, Dumay A, Poirot B, Porcher R, et al. p53 in breast cancer subtypes and new insights into response to chemotherapy. Breast. 2013;22(Suppl 2):S27–9.
21. Niikura N, Sakatani T, Arima N, Ohi Y, Honma N, Kanomata N et al. Assessment of the Ki67 labeling index: a Japanese validation ring study. Breast Cancer. 2014.

Gastric Cancer
DOI 10.1007/s10120-015-0551-7

ORIGINAL ARTICLE

Nuclear PRMT1 expression is associated with poor prognosis and chemosensitivity in gastric cancer patients

Bolag Altan[1] · Takehiko Yokobori[1] · Munenori Ide[2] · Erito Mochiki[3] · Yoshitaka Toyomasu[1] · Norimichi Kogure[1] · Akiharu Kimura[1] · Keigo Hara[1] · Tuya Bai[1] · Pinjie Bao[1] · Masaki Suzuki[1] · Kyoichi Ogata[1] · Takayuki Asao[4] · Masahiko Nishiyama[5] · Tetsunari Oyama[2] · Hiroyuki Kuwano[1]

Received: 26 March 2015 / Accepted: 18 September 2015

Abstract
Background Metastatic and refractory gastric cancer (GC) are associated with a poor prognosis; therefore, the identification of prognostic factors and chemosensitivity markers is extremely important. Protein arginine methyltransferase 1 (PRMT1) may play a role in chemosensitivity/apoptosis induction via activation of the tumor suppressor forkhead box O1 (FOXO1). The purpose of this study was to clarify the expression of and relationship between PRMT1 and FOXO1 to evaluate the applicability of PRMT1 as a prognostic marker and a therapeutic tool in GC.
Methods We investigated the clinical and functional significance of PRMT1 and FOXO1 in 195 clinical GC samples using immunohistochemistry. We performed suppression analysis of PRMT1 using small interfering RNA to determine the biological roles of PRMT1 in chemosensitivity.
Results PRMT1 and FOXO1 in GC samples were predominantly expressed in the nucleus. Patients with lower PRMT1 expression ($n = 131$) had suppressed nuclear accumulation of FOXO1, higher recurrence after adjuvant chemotherapy, and poorer prognosis than those with higher PRMT1 expression ($n = 64$). PRMT1 downregulation in GC cells by RNA interference inhibited cisplatin and 5-fluorouracil sensitivity. The expression of phosphorylated FOXO1 and phosphorylated BCL-2 antagonist of cell death was upregulated in PRMT1 small interfering RNA groups.
Conclusion Our data suggest that the evaluation of PRMT1 expression in GC is a useful predictor of poor prognosis and recurrence after adjuvant chemotherapy. Moreover, these data suggest that PRMT1 is a promising therapeutic tool for overcoming refractory GC.

Keywords Protein arginine methyltransferases · Arginine methyltransferase · Noncoding RNA · Forkhead box O1

B. Altan and T. Yokobori equally contributed to this report.

Electronic supplementary material The online version of this article (doi:10.1007/s10120-015-0551-7) contains supplementary material, which is available to authorized users.

✉ Takehiko Yokobori
bori45@gunma-u.ac.jp

[1] Department of General Surgical Science, Graduate School of Medicine, Gunma University, Maebashi, Gunma, Japan

[2] Department of Diagnostic Pathology, Graduate School of Medicine, Gunma University, Maebashi, Gunma, Japan

[3] Department of Digestive Tract and General Surgery, Saitama Medical Center, Saitama Medical University, Saitama, Japan

[4] Department of Oncology Clinical Development, Graduate School of Medicine, Gunma University, Maebashi, Gunma, Japan

[5] Department of Molecular Pharmacology and Oncology, Graduate School of Medicine, Gunma University, Maebashi, Gunma, Japan

Introduction

Gastric cancer (GC) is an important cause of cancer-related death worldwide [1, 2]. Postoperative adjuvant chemotherapy significantly improves the prognosis of GC patients in comparison with that of nontreated GC patients [3]. However, patients with metastasis or refractory disease after surgery often require intensive adjuvant chemotherapy. To provide optimal treatment for GC, identification of predictors of poor prognosis and chemosensitivity is extremely important. Moreover, it is expected that such markers may also be promising treatment targets.

Published online: 15 October 2015